

MASSACHUSETTS INSTITUTE OF TECHNOLOGY
LINCOLN LABORATORY

DETECTION AND FALSE ALARM PERFORMANCE
OF A PHASE-CODED RADAR WITH POST-MTI LIMITING

R. M. O'DONNELL

Group 43

TECHNICAL NOTE 1975-62

21 NOVEMBER 1975

Approved for public release; distribution unlimited.

LEXINGTON

MASSACHUSETTS

ABSTRACT

This report studies the detection and false alarm performance of the generic type of radar which employs a phase-coded pulse compression and an MTI system followed by limiting. This technique has been referred to as CPACS (Coded Pulse Anti-Clutter System). One specific implementation of the technique was studied in detail. Since the processor employs nonlinear operations, Monte Carlo simulation techniques were used rather than analytical techniques. The results show that for the system simulated there is very poor detection performance in clutter areas with clutter-to-noise C/N greater than 20 dB. For values of C/N greater than 30 dB there is zero detectability of signal, noise or clutter because of limiting in the A/D converters and the limiter after the three-pulse MTI canceller. This is a manifestation of the so-called "black hole effect". Even in a very low C/N environment the processor is 7 dB less than the optimum receiver.

I. Introduction

It is the purpose of this report to study the detection and false alarm performance of the generic type of MTI radar system in Figure 1. In this radar system the transmitted pulse is staggered from pulse-to-pulse and is phase coded with a thirteen-bit Barker Code. The transmitted pulses are staggered in time to increase the unambiguous radial velocity interval and are phase coded to compress the pulse so that backscatter from the ground clutter will be reduced due to the smaller range resolution cell size. Only one channel of the received signal is processed. This signal is sent through a 9-bit A/D converter, a three-pulse canceller, a limiter, a Barker decoder and a detector whereupon the resulting signals are sent through a threshold which is the same for all range-azimuth cells.

Because of the non-linear elements in the processor, a Monte Carlo simulation technique was used to evaluate this type of processor. It was felt that analytical techniques would not be useful because of the non-linear elements in the system. When simulating the clutter, care was taken to include the effects of antenna motion which decorrelates the backscattered clutter from pulse-to-pulse.^[1]

II. Processor Structure

A. A/D Converters

It is assumed that the A/D converters are 9 bits and that if the signal input to the A/D's is greater than $256=2^8$, the output value is +256 and that if the signal input to the A/D's is less than -256, then -256 is output.

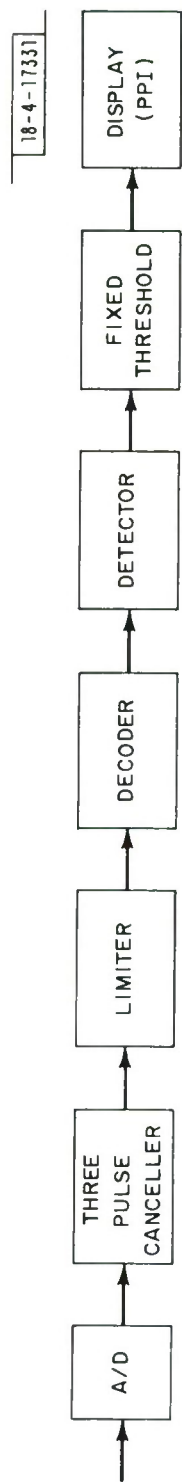


Fig. 1. MTI radar signal processor.

B. Three-Pulse Canceller

It is assumed that the three-pulse canceller may or may not have a feedback mode. The difference equation for the three-pulse canceller without feedback is

$$Y_i(n) = X_i(n-2) - 2 X_i(n-1) + X_i(n) \quad (1)$$

where $Y_i(n)$ is the output for the n th pulse and the i th subpulse* and $X_i(n)$ is the input to the canceller for the n th pulse and i th subpulse. The difference equation for the three-pulse canceller with feedback is given:

$$Y_i(n) = e_i(n) - 2 e_i(n-1) + e_i(n-2) \quad (2)$$

$$e_i(n) = X_i(n) - 1/4 e_i(n-1) - 1/4 e_i(n-2) \quad (3)$$

where $X_i(n)$ and $Y_i(n)$ are defined as in Equation 1.

In actual operation of the radar, the feedback option in the three-pulse canceller is rarely used. Because of this, the feedback option in the MTI circuit was not used when the radar was simulated in this study.

C. Limiter

Next, the pulse passes through a limiter whose properties are

$$Y_i(n) = +1 \text{ for } X_i(n) > 0$$

$$Y_i(n) = 0 \text{ for } X_i(n) = 0$$

$$Y_i(n) = -1 \text{ for } X_i(n) < 0$$

*Each pulse is divided up into 13 subpulses by the Barker Code.

where $X_i(n)$ is the digital voltage input to the limiter for the i th subpulse and the n th pulse, and $Y_i(n)$ is the voltage output from the limiter for the i th subpulse and n th pulse.

D. Decoder

A standard Barker decoder is employed to measure which subpulse the target is in. A block diagram of the decoder is given in Figure 2. With this decoder, the voltages from 13 contiguous subpulse samples are added together after weighting by the Barker codes.

E. Detector

It is assumed that the radar has an envelope detector which extracts the modulation from the carrier frequency.

F. Thresholding

The output of the detector is displayed on PPI after passage through a fixed threshold for all range-azimuth cells.

III. Simulation

A. Generation of Targets, Clutter and Noise

The target voltage at the radar receiver IF is given by

$$V_s(t) = a_i V_s \cos 2\pi f_d t$$

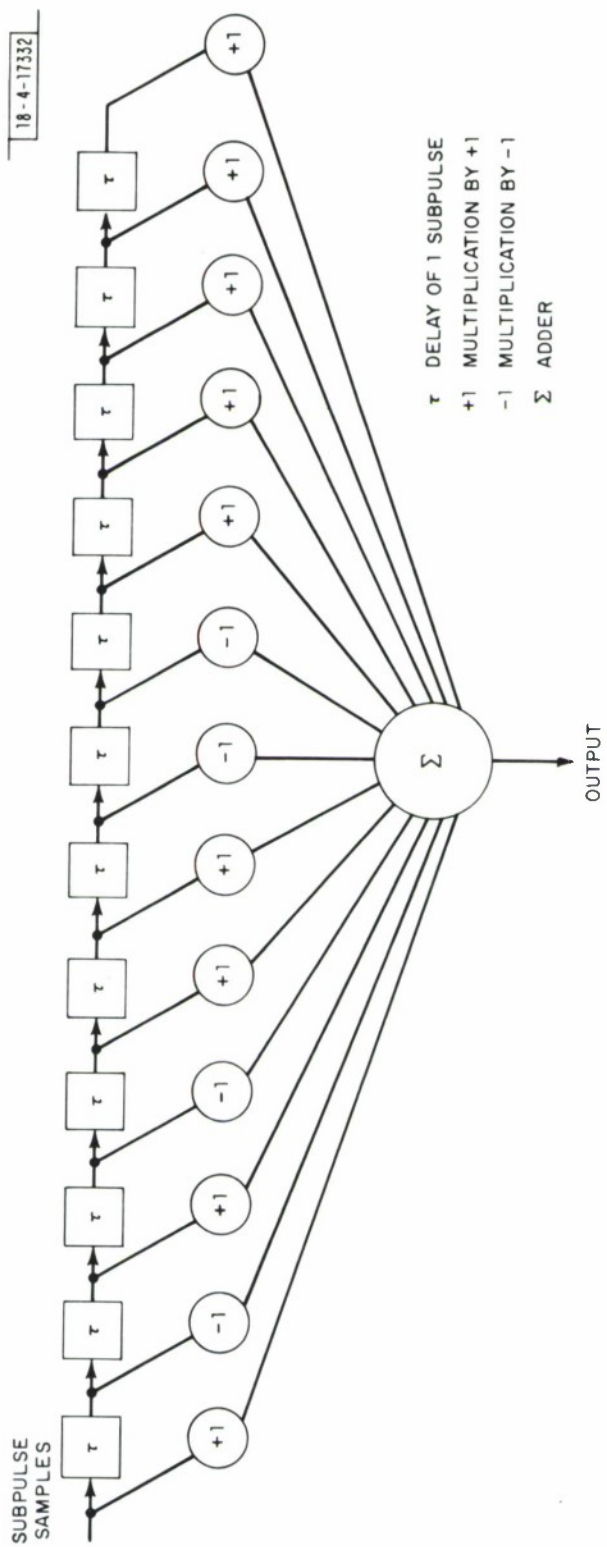


Fig. 2. Block diagram of 13-bit Barker decoder.

where v_s = peak signal voltage
 $f_d = \frac{2v_r}{\gamma}$ = Doppler frequency of target
 a_i = 13-bit Barker code, +1, +1, +1, +1, +1, +1, -1, -1, +1, +1, -1, +1
 v_r = target radial velocity
 γ = wavelength of target
 t = time

Note that the radar does not have an I and Q channel. Because the radar has only one channel, it is subject to the "blind phase" problem which decreases significantly the average detectability of radar. In this simulation the target phase was chosen to be the optimal one. Because of this effect, actual radar will have performance somewhat less than that simulated here.

The target voltage is sampled at the intervals given by one of the two nine-pulse staggers used in the evaluation. The nine-pulse stagger intervals are given in Table 1. The pulse width is assumed to be 6 μ sec and thus the pulse width of the subpulses is .46 μ sec.

Clutter is generated using a program developed at the Laboratory by M. Labitt^[1]. The program generates clutter whose correlation properties from pulse-to-pulse are determined by the scan rate of the antenna, the aperture of the antenna and the wavelength. In this case, the scan rate was one revolution per 12 seconds, an aperture of 14.7 meters and a wavelength of .23 meter (L-band). The clutter return for a given subpulse was taken to be the sum of the return from clutter cells illuminated by all 13 coded subpulses whose time delay matched the delay for the subpulse of interest. The

Table 1
Time Between Pulses (μ sec)

Stagger 1	Stagger 2
2780. μ sec	2820. μ sec
3670.	3720.
2780.	2820.
3330.	3370.
2780.	2820.
2780.	2820.
3570.	3620.
2780.	2820.
2880.	2910.

clutter was assumed to be independent from subpulse-to-subpulse, but correlated partially from pulse-to-pulse due to the scanning of the antenna.

Noise was assumed to be zero mean and Gaussian whose RMS value relative to a least count in the A/D converters was an input parameter.

The RMS clutter voltage and RMS signal voltage were calculated from the input values of clutter-to-noise ratio per subpulse and signal-to-noise ratio per subpulse, and the RMS noise value relative to a least count in the A/D converters.

IV. Simulation & Results

The results of false alarm statistics of the simulation are shown in Figures 3 through 5. Figures 3 through 5 present the probability of false alarm vs threshold setting per subpulse for various clutter-to-noise ratios, threshold settings and values of RMS noise level relative to the least count in the A/D converters. The three-pulse canceller was used without feedback and the first of the two nine-pulse staggers was used. We see from Figure 4 that for very low clutter-to-noise (C/N) levels a threshold of 12 or greater is necessary for a P_{FA} of between 10^{-3} and 10^{-4} . Therefore in the detection results which follow, we choose a threshold of greater than 11 as a criteria for detection. In Figure 6, the probability of detection vs signal-to-noise per subpulse is plotted for various values of C/N. Notice that detection performance degrades significantly for $C/N > 20$ dB. Also for low values of C/N, a signal-to-noise ratio of about 1 dB per subpulse is necessary for detectability. For values of C/N greater than 30 dB, there is almost zero detectability because of the limiting in the A/D's and the limiter after the three-pulse canceller.

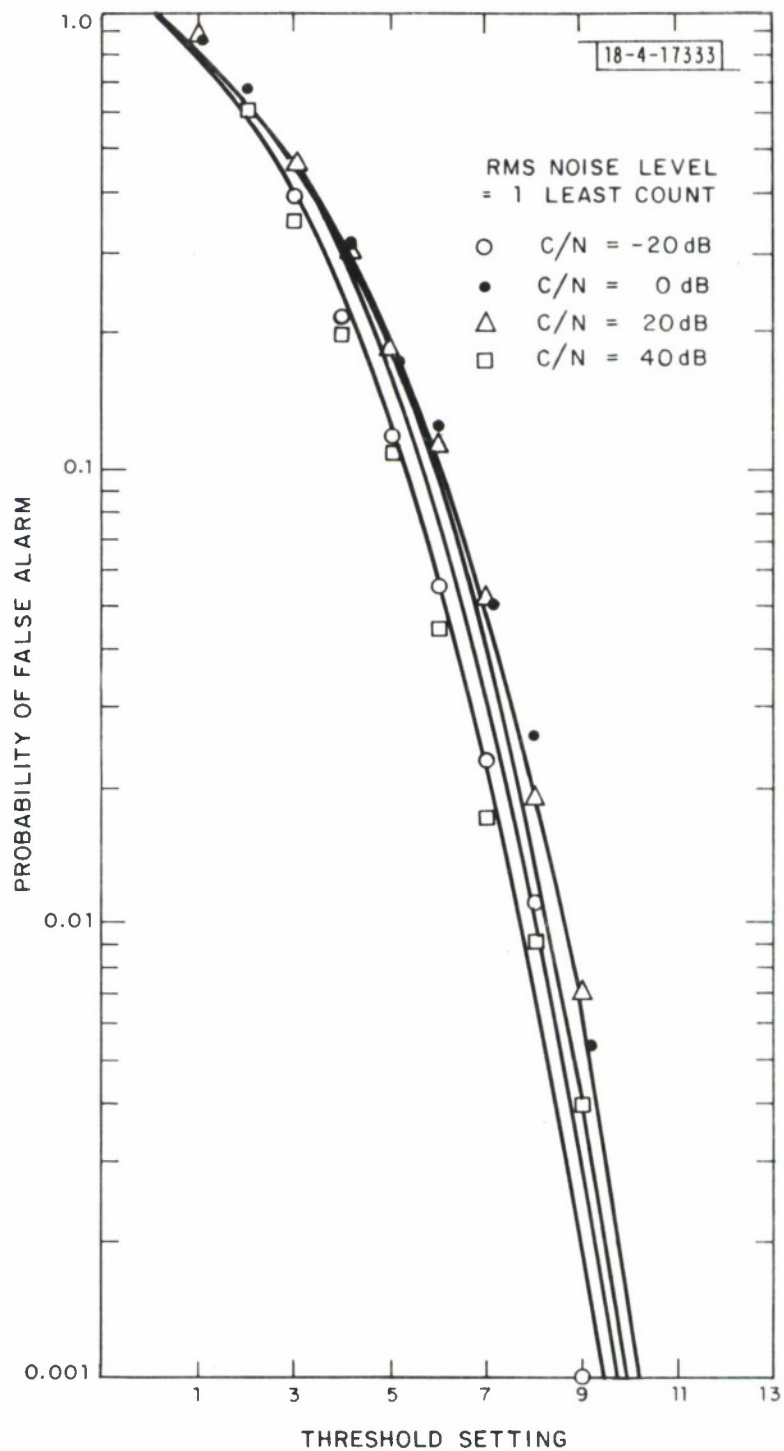


Fig. 3. Probability of false alarm vs threshold setting RMS noise =1 least count.

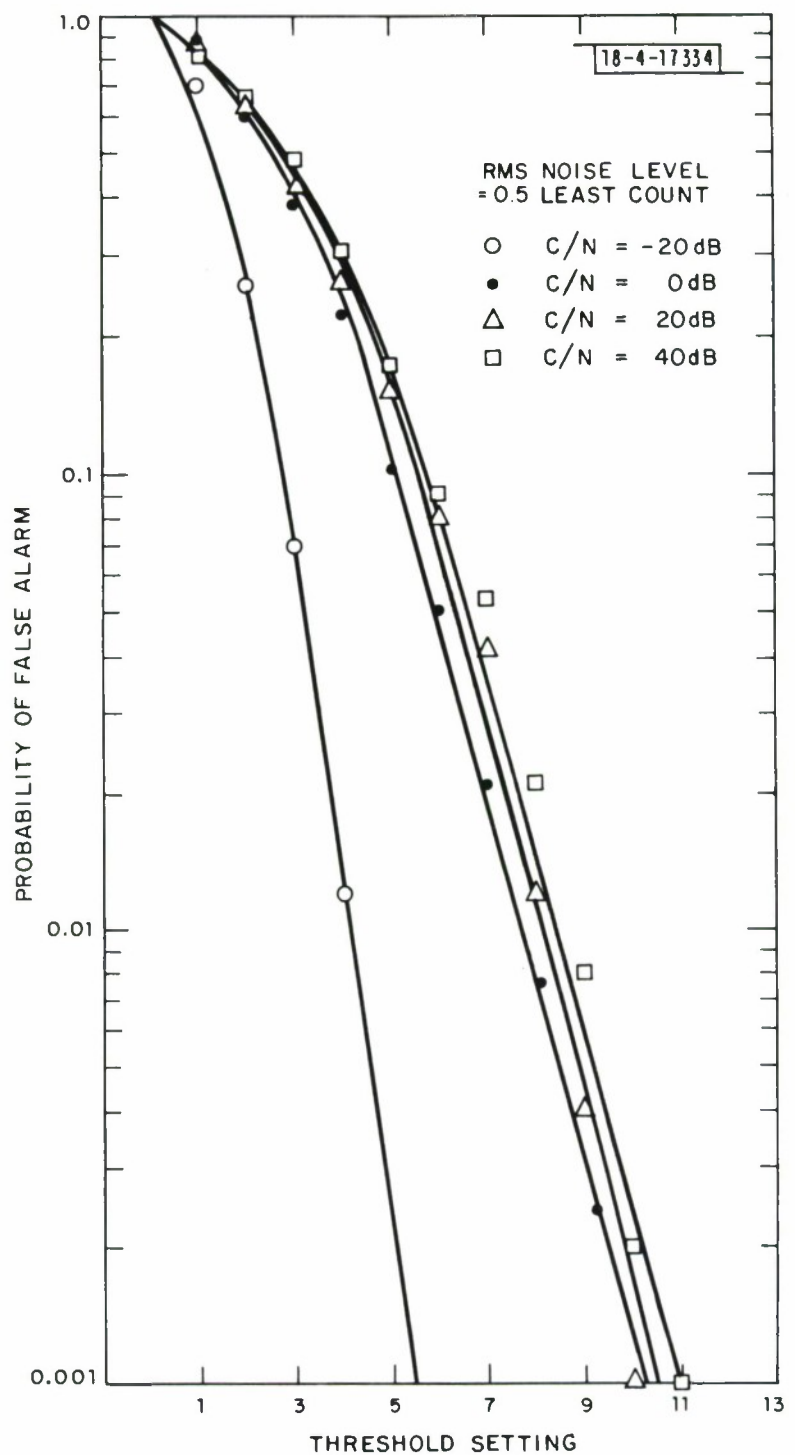


Fig. 4. Probability of false alarm vs threshold setting RMS noise level = 0.5 least count.

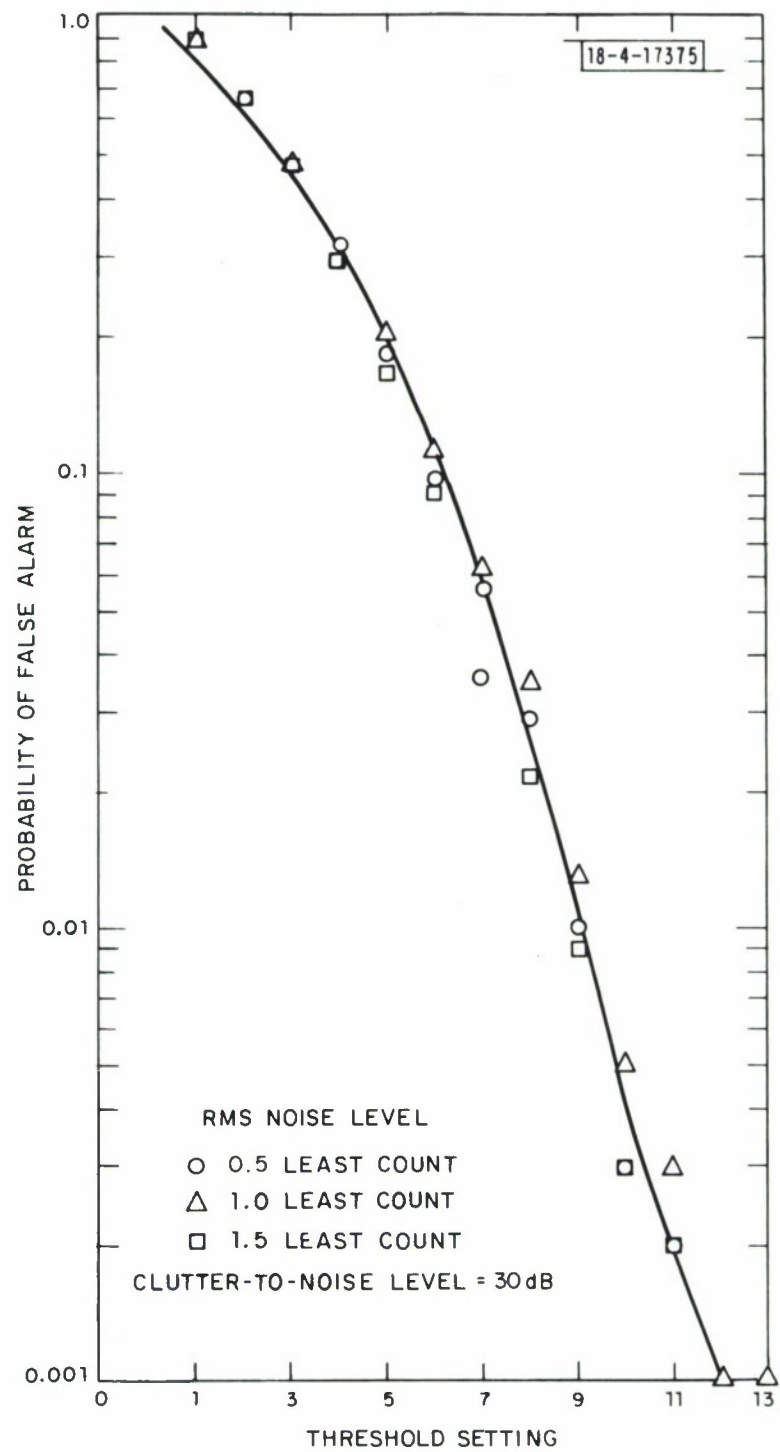


Fig. 5. Probability of false alarm vs threshold setting clutter-to-noise level (C/N) = 30 dB.

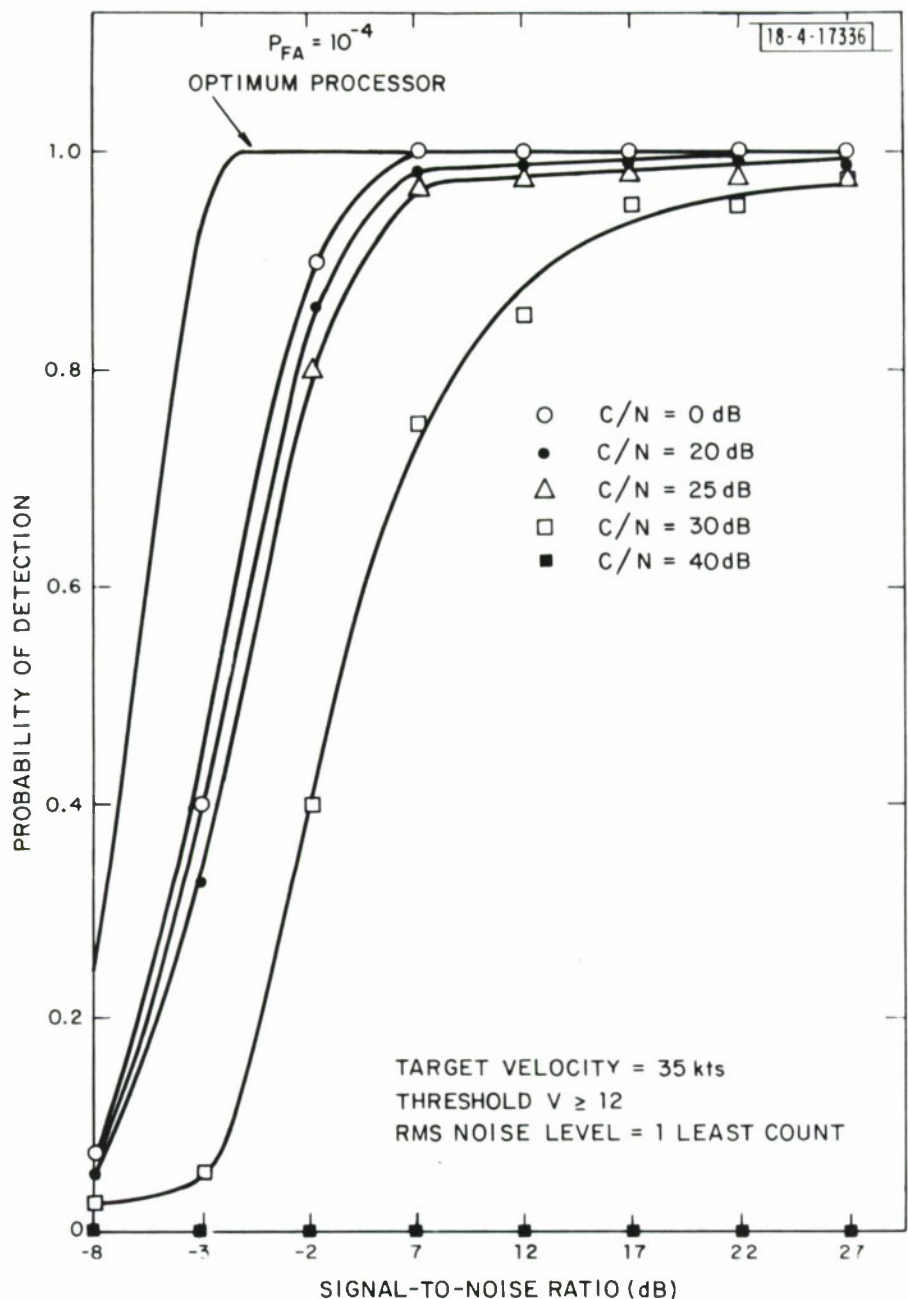


Fig. 6. Probability of detection vs signal-to-noise ratio for optimum processor and simulated MTI radar at various clutter-to-noise ratios.

Thus we see that in the presence of heavy clutter, there is a "black hole effect," that is threshold crossings due targets, clutter, or noise are completely inhibited.

In Figure 6, we have also presented the detection statistics for the optimum processor. This curve is the single pulse P_D vs S/N at $P_{FA} = 10^{-4}$ for a steady target in Gaussian noise. This curve has been offset by 15.35 dB, 11.1 dB due to the gain of the 13-bit Barker code and 4.25 dB due to integration gain of the three-pulse canceller. It is evident that even for a very low clutter-to-noise level environment this processor is at least 4 dB worse than the optimum receiver. Also, when the signal was generated the phase of the signal voltage was set equal to zero and the in-phase component (I channel) used. The assumption neglected the effects of blind phases of the target. This loss is about 3 dB. Thus, we see that overall, this type of MTI processor has about 7 dB less performance than the optimum processor.

In Figure 7, the probability of detection vs signal-to-noise ratio for $C/N = 30$ dB is presented for three values of RMS noise voltage relative to a least count in the A/D converters. It is apparent that the higher the RMS noise voltage, the lower the performance of the system. In Figure 8, detection statistics are presented for three values of target radial velocity. The two values of target speed which bracket the 35-knot value show degraded performance as expected. The 35-knot speed corresponds to the 1/2 the first blind speed in a constant PRF system with pulse interval of about 3 msec, while 69 knots is at the first blind speed. Although the detection performance

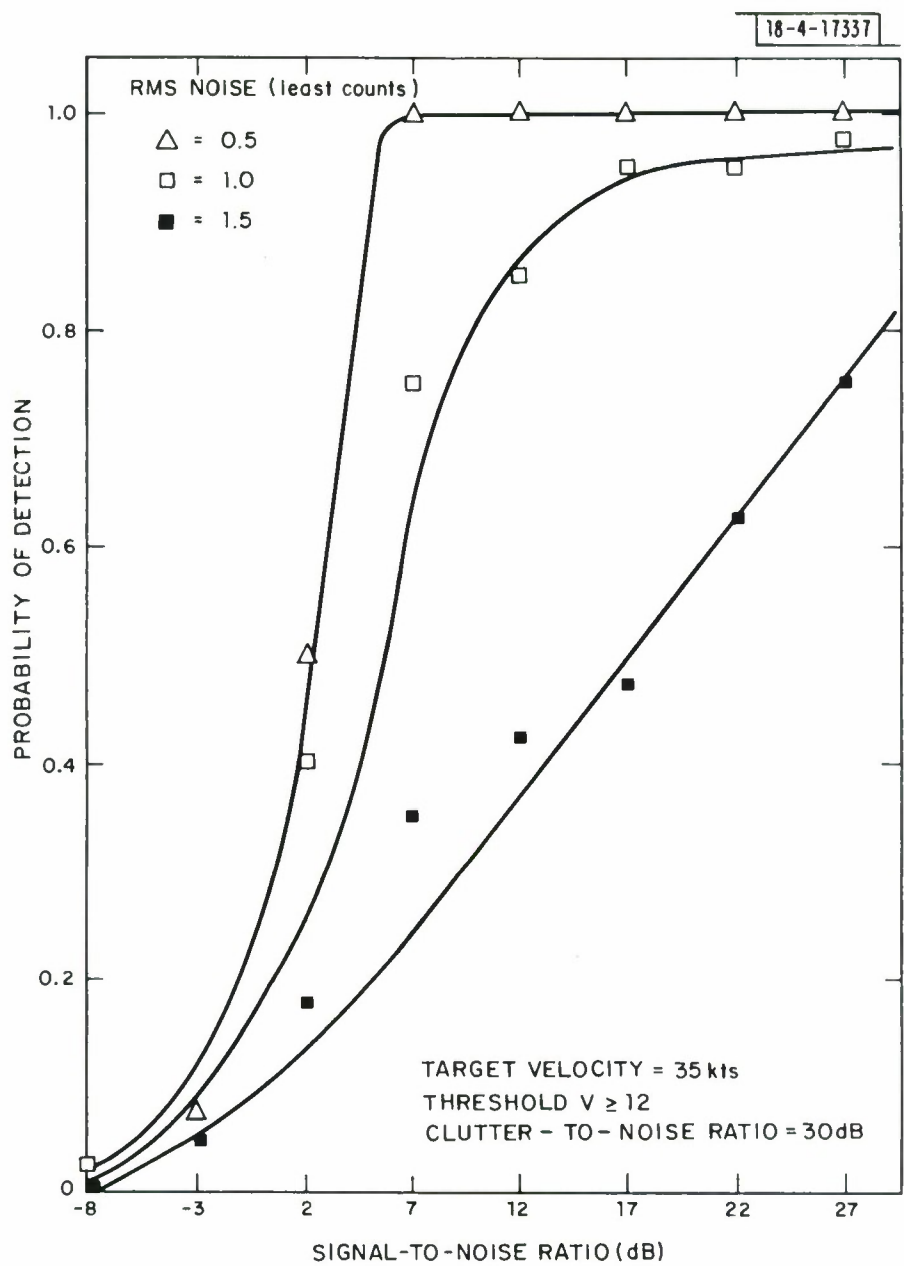


Fig. 7. Probability of detection vs signal-to-noise ratio for various RMS noise levels.

is degraded significantly at the "blind speed", since we are using a staggered PRF, performance is not reduced to zero.

Lastly, an attempt was made to study the effect of changes in the limiter following the three-pulse canceller. The limiter was modified to have the following properties.

$$\begin{aligned} Y_i(n) &= +1 \text{ for } X_i(n) > 2 \\ Y_i(n) &= 0 \text{ for } |X_i(n)| < 2 \\ Y_i(n) &= -1 \text{ for } X_i(n) < -2 \end{aligned}$$

A graph of false alarm probability vs threshold setting for an RMS noise value of 1 least count is presented in Figure 9 for several values of C/N. For this type of limiting, the false alarms are bunched down at the lower ends of threshold values for low values of C/N more so than with the normal limiter. Figure 10 presents the detection statistics for this limiter with a thresholding criteria of the voltage greater than 11 to declare a target. These results show slightly poorer detectability for this limiter than with the normal one.

V. Summary

The detection performance of the radar is good for clutter-to-noise (C/N) ratios less than 20 dB, and a signal-to-noise ratio of 1 dB per subpulse is necessary for good detectability. For C/N greater than 20 dB, there is serious degradation in detection performance. For values of C/N greater than 30 dB, there is almost zero detectability of targets, clutter, or noise because of the limiting in the A/D converters and in the limiter after the three-pulse

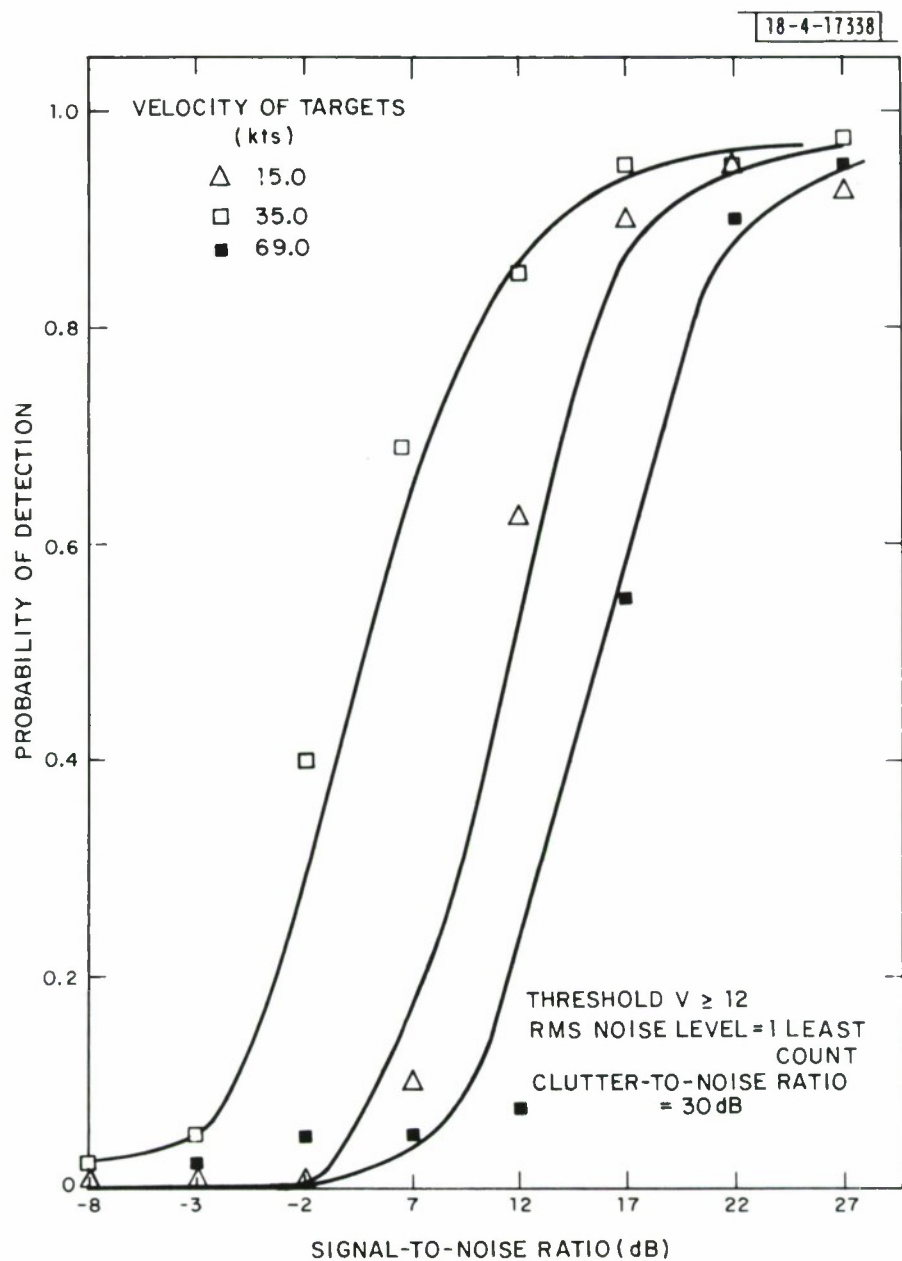


Fig. 8. Probability of detection vs signal-to-noise ratio for various target velocities.

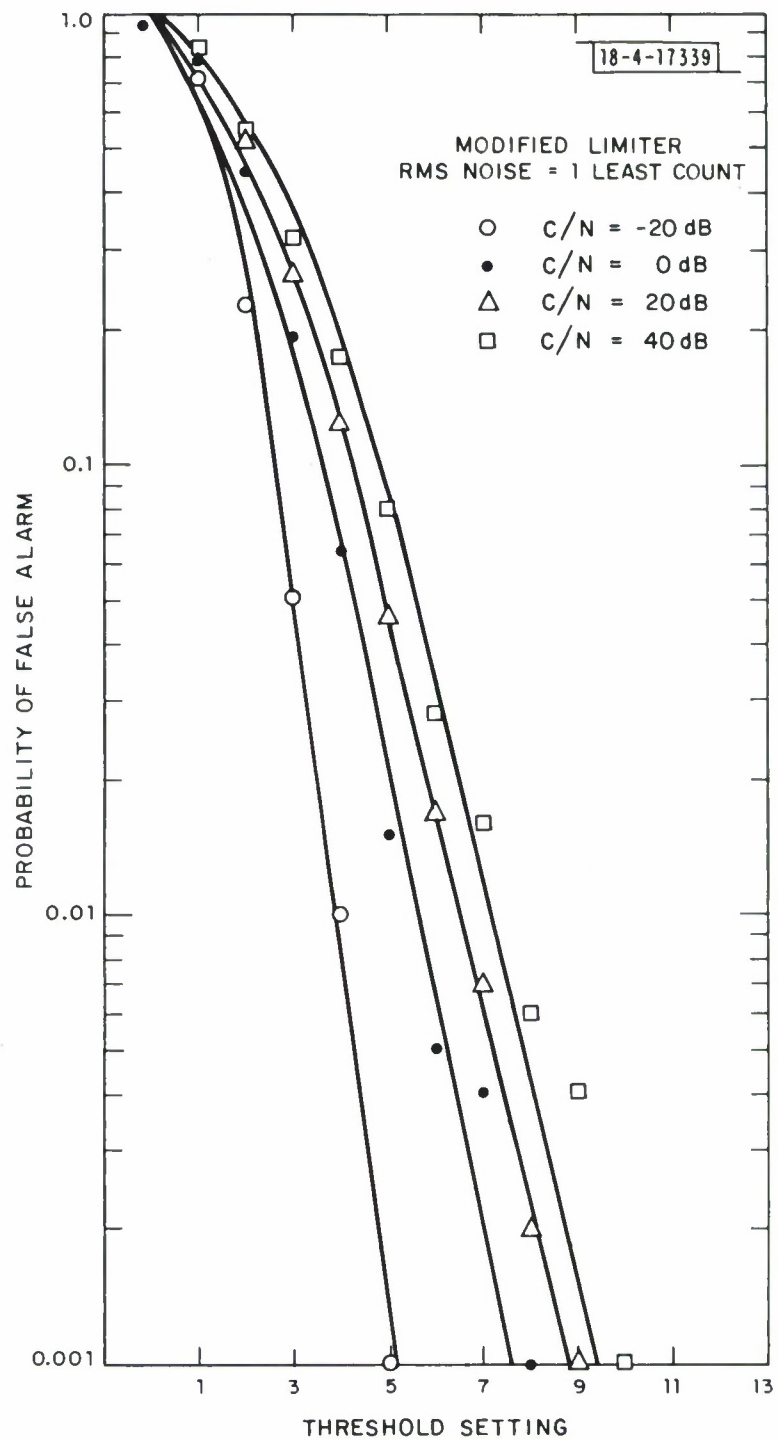


Fig. 9. Probability of false alarm vs threshold setting for MTI radar with modified limiter.

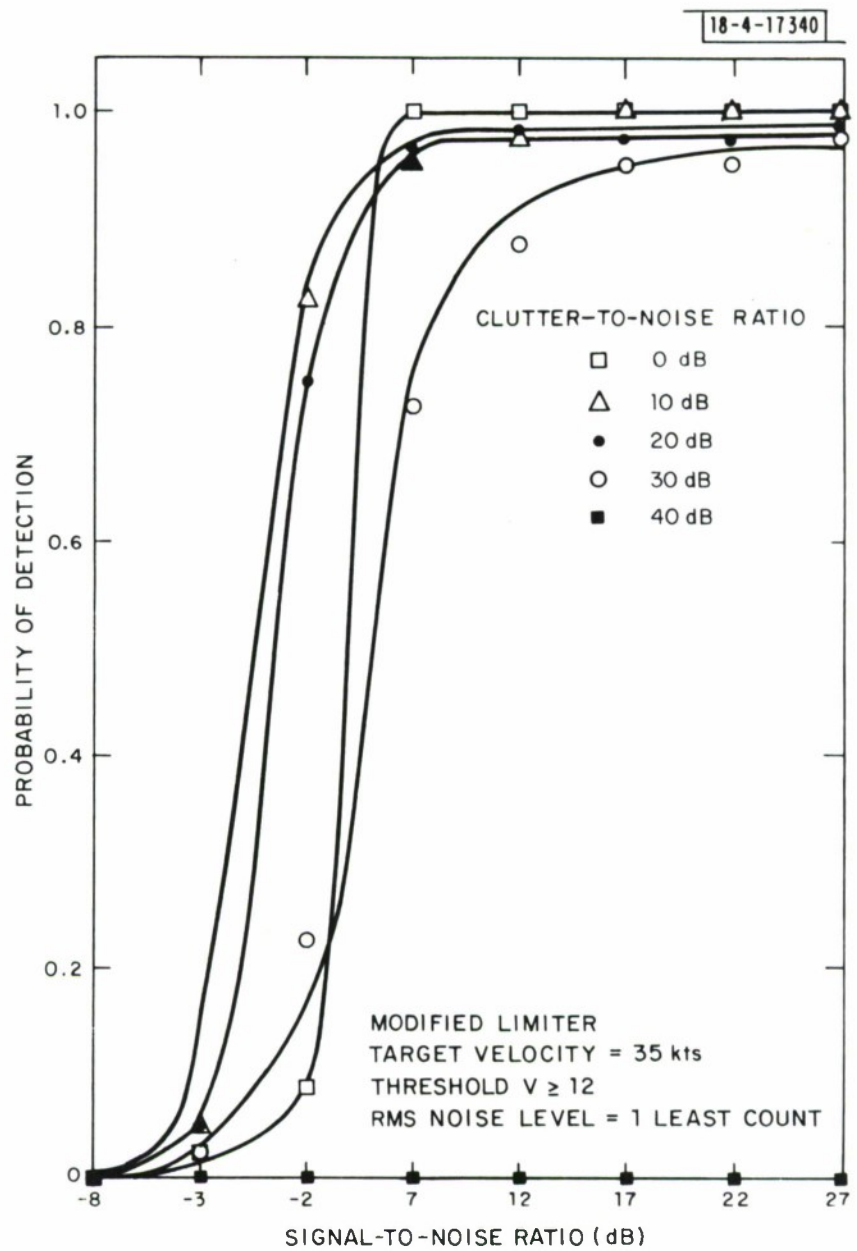


Fig. 10. Probability of detection vs signal-to-noise ratio for various clutter-to-noise ratios.

canceller. Even in a very low clutter-to-noise level environment, this radar processor is at least 7 dB worse than the optimum receiver.

References

1. M. Labitt, "The Generation of Scanning Clutter," private communication.
2. F. Nathanson, Radar Design Principles (McGraw-Hill, New York, 1969)

UNCLASSIFIED

SECURITY CLASSIFICATION OF THIS PAGE (When Data Entered)

DEPARTMENT OF THE AIR FORCE
HEADQUARTERS ELECTRONIC SYSTEMS DIVISION (AFSC)
HANSOM AIR FORCE BASE, MASSACHUSETTS 01731



REPLY TO
ATTN OF:

TML (Lincoln Lab)

3 December 1975

SUBJECT: ESD-TR-75-318, dtd 21 Nov 75, "Detection and False Alarm Performance
of a Phase-Coded Radar with Post-MTI Limiting"

TO: DDC/Air Force Liaison Representative
Cameron Station
Alexandria, VA 22314

1. I certify that the subject TR has been reviewed and approved
for public release by the controlling office and the information
office in accordance with AFR 80-45/AFSC Sup 1. It may be made
available or sold to the general public and foreign nationals.

2. Distribution statement A appears on the subject TR and the
DD Form 1473 as required by AFRs 80-44 and 80-45.

FOR THE COMMANDER

/s/
EUGENE C. RAABE, Lt Colonel, USAF
Chief, Lincoln Laboratory Project Office

Atch

ESD-TR-75-318
(12 copies)